LPV/LFT Control Design Equipped with a Command Governor for Different Steering Scenarios

Dimitrios Kapsalis, Olivier Sename, Vicente Milanes, John Jairo Martinez Molina

To cite this version:

HAL Id: hal-03227095

https://hal.univ-grenoble-alpes.fr/hal-03227095

Submitted on 16 May 2021

LPV/LFT Control Design Equipped with a Command Governor for Different Steering Scenarios

Dimitrios Kapsalis [*,**] **Olivier Sename** [**] **Vicente Milanes** [*]
John J. Martinez [**]

[*] *Research Department, Renault SAS, 1 Avenue de Golf, 78280 Guyancourt, France. (e-mail: {dimitrios.kapsalis, vicente.milanes}@renault.com).*
[**] *Univ. Grenoble Alpes, CNRS, Grenoble INP, GIPSA-Lab, 38000, (e-mail:{olivier.sename, john-jairo.martinez-molina}@grenoble-inp.fr)*

Abstract: This paper presents a Linear Parameter Varying (LPV) based approach to handle different steering scenarios for autonomous vehicles. The proposed methodology consists of the design of a fast and performant LPV/LFT controller which can track the generated yaw rate reference, for speed operating range, for lane tracking and smooth/fast lane changes. The handling of a dynamic maneuver is achieved by a Command Governor (CG), which feeds the updated LPV/LFT closed loop system with a "virtual" yaw rate reference. This virtual signal is the solution of an online receding horizon optimization problem, meeting simultaneously safety bounds for the steering of the vehicle. The efficiency of the suggested methodology is illustrated by simulation results for parameters of an automated Renault Zoe.

Keywords: Automotive control, Autonomous Vehicles, Lateral Control, LPV/LFT, Command Governor

1. INTRODUCTION

Automated vehicles consist of multiple cooperative systems that have to be able to perform under different scenarios. Vehicle control is the component that defines the behavior of the vehicle for a given task, taking into account constraints, performance criteria and the presence of uncertainties (Paden et al. (2016)).

One of the most significant tasks is the steering of the vehicle. Among steering control techniques are vision-based algorithms where control points located at a look ahead distance in front of the vehicle are tracked. The tracking, for a range of speed considered as a varying parameter, is achieved either by minimizing a lateral error (Taylor et al. (1999)) or by following a yaw rate reference (Tan and Huang (2014)).

Linear Parameter varying (LPV) control emerged as a way to treat systems which include an external parameter that is varying with respect to time but also is measured at every instant. LPV theory has been demonstrated successfully to multiple applications in aerospace, automotive and robotics Hoffmann and Werner (2015); Biannic et al. (1997); Saupe and Pfifer (2012); Marcos et al. (2015); Kapsalis et al. (2020).

On the other hand, reference and command governors (RG and CG) are add-on schemes that supervise the operation of the closed-loop system. This is achieved by solving in real time a linear (for the case of RG) or a QP (for CG) optimization problem where a new virtual reference feeds the system, for which the states of the system do not violate some convex constraints (see Garone et al. (2017)).

This paper at first, presents the design of a yaw rate tracking LPV/LFT controller, considering as varying parameter the lon-

gitudinal speed of the vehicle. As it can be seen in simulation results, the controller can perform well during steering for lane tracking and smooth lane changes.

However, that fast controller is not able to achieve all the required tasks as a dynamic maneuver. The reason is that it leads the vehicle to the loss of control cause of unwanted nonlinear dynamics which are based on the saturation of the lateral forces (Pacejka (2005)). Beal and Gerdes (2012) introduced safe handling constraints on the yaw rate and the side slip angle of the vehicle which are utilized in an MPC framework to control the vehicle at its limits.

In this paper, these safe bounds are exploited and steering wheel angle maximum values are obtained. Taking the varying speed at every instant, the LFT matrices are updated online feeding the CG with the steering wheel angle constraints. Through that CG formulation, the LPV/LFT closed-loop system is restricted to satisfy these bounds and making the maneuver feasible.

The rest of the paper is structured as follows. Section 2 presents the augmented vehicle model used for the LPV/LFT controller synthesis in section 3. Section 4 shows the formulation and the design of the CG, as well as the constraints computation. Section 5 and 6 presents the simulation results for the cases of lane tracking/change and for the fast maneuver respectively.

2. VEHICLE'S LATERAL DYNAMICS

In this paper, for control design purpose, the bicycle model (See Rajamani (2011)) is considered to describe the vehicle's lateral motion (lateral speed and yaw rate). Considering the velocity of the vehicle v_x as external varying parameter, a steering controller can be designed regardless of the longitudinal motion of the car. Note that this decoupling of the longitudinal and lateral control is quite usual in that (industrial) context.

Fig. 1 shows the bicycle model which consists of the front and rear wheels (assuming the left/right symmetry). v_x, v_y are the longitudinal and lateral speeds, F_{yf} and F_{yr} are the lateral tire forces, L_f, L_r are the distances of the front and rear wheel from the center of gravity respectively. $\dot{\psi}$ is the yaw rate of the car. α_f, α_r are the tire side-slip angles of the front and rear wheels respectively. β is the side slip angle of the vehicle body. δ is the steering wheel angle and C_f, C_r are the front and rear cornering stiffness.
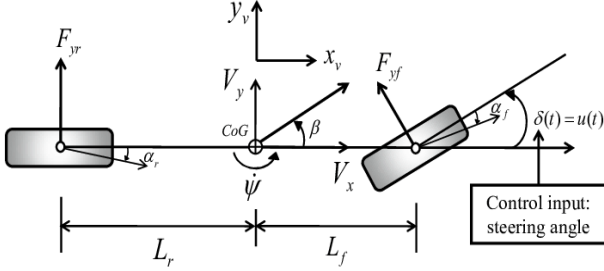

Fig. 1. Two wheeled bicycle model depicting the lateral dynamics of the vehicle.

Assuming small side slip and steering angles, the bicycle model is given in a linear state space form as follows (see for instance Corno et al. (2020)):

$$\dot{x}(t) = Ax(t) + Bu(t)$$
$$y(t) = Cx(t) \tag{1}$$

with, $A = \begin{bmatrix} -\dfrac{C_f + C_r}{mv_x} & -v_x + \dfrac{C_r L_r - C_f L_f}{mv_x} \\ \dfrac{-L_f C_f + L_r C_r}{I_z v_x} & -\dfrac{L_f^2 C_f + L_r^2 C_r}{I_z v_x} \end{bmatrix}$, $B = \begin{bmatrix} \dfrac{C_f}{m} \\ \dfrac{L_f C_f}{I_z} \end{bmatrix}$

and $C = [0\ 1]$.

The state space vector is $x(t) = \begin{bmatrix} v_y \\ \dot{\psi} \end{bmatrix}$ and the input $u(t) = \delta$ is the steering wheel angle.

Note that the steering command is applied to the vehicle by an actuator which has been identified in the Renault test car as a second order model with a time delay. The actuator model is the one shown below:

$$G_{act} = \frac{k}{s^2 + 2\zeta\omega_n s + \omega_n^2} e^{-T_d s} \tag{2}$$

where k, ζ, ω_n and T_d are the static gain, the damping, the natural frequency and the time-delay respectively. For control design the time delay is modeled by a second order Padé approximation. Therefore, the identified fourth order model is expressed in a state space form as presented below:

$$\dot{x}_{act}(t) = A_{act}x_{act}(t) + B_{act}\delta(t)$$
$$\delta_{act}(t) = C_{act}x_{act}(t) \tag{3}$$

where $x_{act} \in \mathbb{R}^4$ is the vector expressing the states of the actuator, $A_{act} \in \mathbb{R}^{4\times4}$, $B_{act} \in \mathbb{R}^{4\times1}$, $C_{act} \in \mathbb{R}^{1\times4}$ are the systems matrices and $\delta_{act} \in \mathbb{R}$ is the output.

The two systems (1), (3) are connected in series to form an augmented state space model that will be considered for the synthesis of the steering controller.

$$\begin{cases} \dot{x}_f(t) = A_f x_f(t) + B_f u(t) \\ \quad y(t) = C_f x_f(t) \end{cases} \tag{4}$$

where, $x_f(t) = \begin{bmatrix} x(t) \\ x_{act}(t) \end{bmatrix} \in \mathbb{R}^6$ is the extended state vector,

$A_f = \left[\begin{array}{c|c} A & BC_{act} \\ \hline 0 & A_{act} \end{array}\right] \in \mathbb{R}^{6\times6}$, $B_f = \begin{bmatrix} 0 \\ B_{act} \end{bmatrix} \in \mathbb{R}^6$

and $C_f = [C\ 0] \in \mathbb{R}^{1\times6}$ are the extended system matrices.

3. LFT CONTROLLER DESIGN

This section presents the design of the LFT controller, taking the speed as a varying parameter, that can perform sufficiently for the cases of lane tracking and during a smooth lane change.

3.1 LPV/LFT Model Formulation

The augmented model (4) is a LPV model considering the velocity of the car $\rho(t) = v_x(t)$ as a bounded varying parameter in the system matrix $A_f(\rho(t))$.

$$\dot{x}_f(t) = A_f(\rho(t))x_f(t) + B_f u(t)$$
$$y(t) = C_f x_f(t) \tag{5}$$

In this study we have chosen to represent the above LPV system (5) in the Linear Fractional Transformation (LFT) form (Packard (1994)). Indeed such a representation is very convenient when the state matrices have a rational dependency on the parameter ρ (as here for v_x) (Cockburn and Morton (1997)). Note that this may allow to reduce the conservatism of the polytopic approach (see for instance Kapsalis et al. (2021)).

The LFT plant (Fig. 2) is an interconnection of two parts: a Linear Time-Invariant system M and a diagonal matrix $\Delta(\rho) = \rho I_{4\times4}$ that includes all the appearances of the varying parameter ρ in the varying parameter matrix $A_f(\rho)$. The input ω_Δ and output z_Δ (where $\omega_\Delta = \Delta(\rho)z_\Delta$) are the fractional feedback variables which describes how the parameter ρ enters in the vehicle dynamics. This allows to pull out the varying parameters from the LTI part.
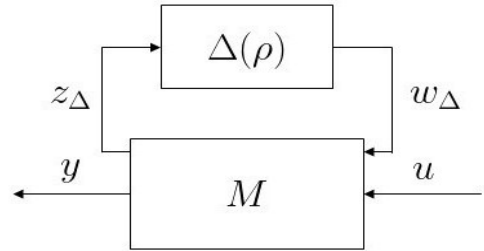

Fig. 2. LFT open-loop system

3.2 Dynamic Output LFT/H_∞ Controller Design

The automatic steering control system is based on tracking a yaw-rate reference $r(t)$ computed at a target point, ahead of the vehicle at a look-ahead distance L, located onto the reference trajectory (See Tan and Huang (2014)). The designed steering controller has to be fast enough but also provide comfort at the same time.

To achieve the aforementioned objectives, some weighting functions are selected to tune properly the tracking controller, where the yaw-rate tracking H_∞ control structure is presented in Fig. 3.
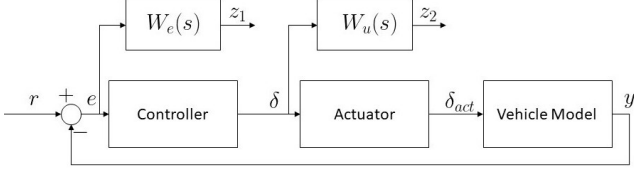
Fig. 3. Control structure for yaw-rate tracking using H_∞ weighting functions.

The first order filters $W_e(s)$ and $W_u(s)$ are selected to ensure tracking of the yaw rate reference (through $W_e(s)$), while handling the actuator limitation thanks to $W_u(s)$ (Skogestad (2007)).

The template functions are chosen as explained below:

- $W_e(s) = \dfrac{s/M_e + \omega_e}{s + \omega_e \varepsilon}$, where $\omega_e = 3 rad/s$ is the bandwidth for fast tracking of the reference. $M_e = 2(6db)$ is chosen to ensure robustness and $\varepsilon_e = 0.001$ which corresponds to the steady state tracking error.

- $W_u(s) = \dfrac{s + \omega_u/M_u}{\varepsilon_u s + \omega_u}$, where $\omega_u = 10 rad/s$ is the bandwidth of the controller and have a smooth steering wheel angle change. $M_u = 2(6db)$ is chosen in order to satisfy the saturation limits of the controller and $\varepsilon_u = 0.1$ which is the roll-off frequency for better noise attenuation.

From the plant model and the weighting functions the control scheme in Fig. 3 is converted into the general control configuration in Fig. 4, where P is the LTI part of the LFT form of the generalized plant, including the controlled output vector $z = [z_1\ z_2]^T$ and the exogenous input r.
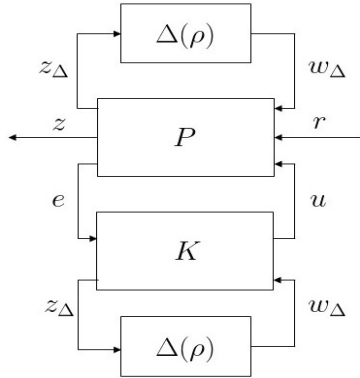

Fig. 4. LFT plant of the augmented vehicle model

The H_∞ control problem to be solved is then formulated as follows : find a controller K such that the LPV/LFT controller $F_l(K, \Delta(\rho))$, where F_l denotes the lower LFT representation, satisfies :

- the closed-loop system in Fig. 4 is internally stable for all parameter trajectories ρ
- The induced $\mathscr{L}_2$-norm between r and z satisfies

$$sup \frac{\|z\|_2}{\|r\|_2} < \gamma_\infty, (\gamma_\infty > 0, \text{ to be minimized})$$

The above problem can be solved through the appropriate Linear Matrix Inequalities as detailed in Apkarian and Gahinet

(1995). Here the LFT controller is computed using the toolbox LPVTools (Hjartarson et al. (2015)) for $v_x \in [5, 25] m/s$,. The optimal attenuation level reached is $\gamma = 1.66$. Fig. 5, 6 depict the frequency response of the closed-loop system in comparison with the template functions $W_e(s)$ and $W_u(s)$.
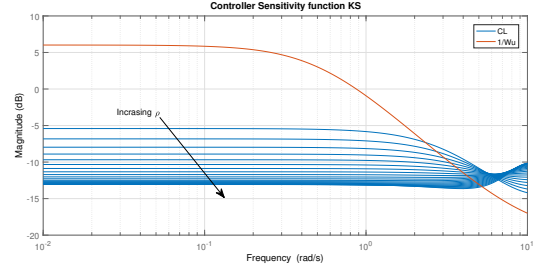

Fig. 5. Controller Sensitivity function of the closed-loop system for different values of the parameter ρ
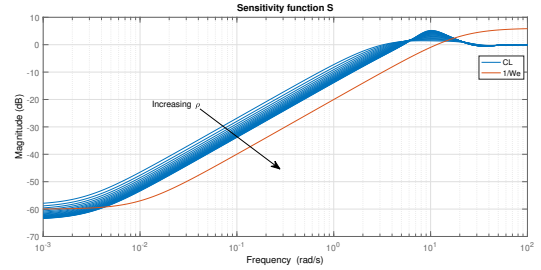

Fig. 6. Sensitivity function of the closed-loop system for different values of the parameter ρ

4. COMMAND GOVERNOR DESIGN FOR EVASIVE MANEUVER

The designed controller is a fast one that can track well a varying reference. However, when an abrupt maneuver is required, that controller will lead the vehicle to loss of control. (Pacejka (2005)). In the sequel, safe bounds on the steering wheel angle of the controller are obtained and the the CG is designed to achieve a fast maneuver.

4.1 "Safe" region of lateral forces

The bicycle model (Rajamani (2011)) is based on the linear approximation of the lateral forces applied to the tires, and can be expressed as follows:

$$\begin{aligned} F_{yf} &= C_f \alpha_f \\ \alpha_f &= \delta - \beta - \frac{L_f \dot\psi}{v_x}, \\ F_{yr} &= C_r \alpha_r \\ \alpha_r &= -\beta + \frac{L_r \dot\psi}{v_x} \end{aligned} \tag{6}$$

In reality, the linear approximation stands till some maximum value of the side slip angles $\alpha_{f,max}$ and $\alpha_{r,max}$ after which the forces start to saturate (Pacejka (2005)). Beal and Gerdes (2012) then define safe envelopes for path tracking as maximum bounds for β and $\dot\psi$ as such:

$$\begin{aligned} \dot\psi_{max} &= \frac{C_r \alpha_{r,max}(1 + L_f/L_r)}{mv_x} \\ \beta_{max} &= a_{r,max} + \frac{L_r \dot\psi}{v_x} \end{aligned} \tag{7}$$

where g is the acceleration due to gravity.

For these maximum values, the maximum "safe" steering wheel angle is defined for which the vehicle can perform a maneuver without loss of control. Combining (6) and (7), the maximum command action is the one below:

$$\delta_{max} = a_{f,max} + \beta_{max} + \frac{L_f \dot{\psi}_{max}}{v_x} \qquad (8)$$

These computed bounds will be used in the optimization problem for the design of the command governor.

4.2 Command governor design for the LPV/LFT system

This subsection presents the Command Governor design for the closed-loop system to enable the vehicle to perform an evasive maneuver. The proposed algorithm is a receding horizon optimization problem solved online by QP programming.

Firstly, the input-output mapping of the the bicycle model (1) is written under LFT form by the upper LFT interconnection:

$$y = F_u(V, \Delta(\rho))\delta \qquad (9)$$

where V is the LTI system of the LFT form of the bicycle model and F_u denotes the upper LFT representation.

In the sequel, the closed-loop LPV model is obtained under the LFT form by interconnecting the vehicle model (9) and the designed LFT controller as such:

$$\mathscr{CL}(V, K, \Delta(\rho)) = F_l(F_u(V, \Delta(\rho)), F_l(K, \Delta(\rho))) \qquad (10)$$

In that way, the actuator dynamics are omitted from the closed-loop system in order to reduce the prediction variables and consequently the optimization problem is faster for real-time implementation. The discretized LFT closed-loop model of (10) for sampling time T_s, is presented below as such:

$$\begin{aligned} x_{cl}(k+1) &= A_{cl}(\rho)x_{cl}(k) + B_{cl}(\rho)r(k) \\ y_{cl}(k) &= C_{cl}(\rho)x_{cl}(k) + D_{cl}(\rho)r(k) \end{aligned} \qquad (11)$$

where $x_{cl}(k) = \begin{bmatrix} x(k) \\ x_K(k) \end{bmatrix} \in \mathbb{R}^{10}$ is the closed-loop state space vector, $y_{cl}(k) = \begin{bmatrix} \dot{\psi}(k) \\ \delta(k) \end{bmatrix} \in \mathbb{R}^2$ the closed-loop output vector and the LPV/LFT matrices $A_{cl}(\rho) \in \mathbb{R}^{10 \times 10}, B_{cl}(\rho) \in \mathbb{R}^{10}, C_{cl}(\rho) \in \mathbb{R}^{10}, D_{cl}(\rho) \in \mathbb{R}^2$, given the measured parameter ρ on-line, are updated similarly as the LFT controller in (16).

A Command Governor is designed for the system (11) as a solution to perform an abrupt maneuver. In real time it modifies the yaw-rate reference $r(k)$ by solving a constrained optimization problem and feeding the controller with a virtual reference $v(k)$ for which the constraints are respected throughout a prediction horizon N.

Furthermore, the command governor is fed with the updated LPV/LFT matrices as well as the estimated states $\hat{x}_{cl}(k)$ by an LTI observer designed for the closed-loop system (11) where the parameter ρ has nominal value, i.e $\rho = 15m/s$ (Fig. 7).

As state constraints are chosen:

$$\begin{aligned} |\delta(k)| &<= \delta_{max} \ i.e, \\ |C_K(\rho)x_K(k)| &<= \delta_{max} \end{aligned} \qquad (12)$$

in order to keep the vehicle inside the "safe" region as explained. Furthermore, the slew rate of the virtual reference is

restrained by an upper limit $\mathscr{D}_v$ so as to avoid the overshoot of the controller steering angle.
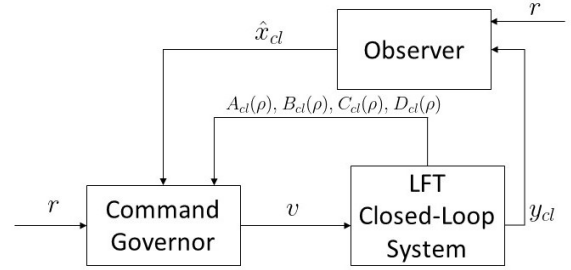

Fig. 7. Full control-scheme including the command governor

All the above constraints and model formulation lead to the quadratic programming problem, where constraint fulfillment and tracking performance is evaluated (Kogiso and Hirata (2006)).

$$\begin{aligned} \underset{v(k)}{\text{minimize}} \quad & J = |v(k) - r(k)|^2 + \sum_{i=1}^{N}(\dot{\psi}(k+i) - r(k))^2 \\ \text{subject to} \quad & x_{cl}(k+1+i) = A_{cl}(\rho)x_{cl}(k+i) + B_{cl}(\rho)v(k), \\ & E(\rho)x_{cl}(k+i) \preceq D, \\ & |v(k)| \le r(k), \\ & |v(k) - v(k-1)| \le \mathscr{D}_v, \\ & \forall i = 1,..,N \end{aligned}$$
$$(13)$$

5. APPLICATION ON LANE CHANGE AND LANE TRACKING.

The designed LPV/LFT controller, as explained previously, can be applied on the scenarios where the vehicle has to perform a) lane change and b) lane tracking.

This section presents the simulation results which has been carried out using a reliable Renault Simulator, where the vehicle's model parameter of (1) correspond to a Renault Zoe. During lane-change a smooth transition from one lane to another is required. For that reason, it is enough to choose the look-ahead distance L "further" from the vehicle and generate a smaller yaw-rate reference. On the contrary, during lane-tracking the look-ahead distance L is chosen "closer" to the vehicle for a higher bandwidth.

First, the steering system accepts command at $T_s = 0.01s$. Consequently, the synthesized LFT controller is discretized for that sampling period. The LTI system of the discretized LFT controller is denoted as:

$$K(z) = \begin{pmatrix} D_{K_{11}} & D_{K_{1\Delta}} \\ D_{K_{\Delta 1}} & D_{K_{\Delta\Delta}} \end{pmatrix} + \begin{pmatrix} C_{K_1} \\ C_{K_\Delta} \end{pmatrix}(zI - A_K)^{-1}(B_{K_1} \ B_{K_\Delta}) \quad (14)$$

The real-time implementation of the discretized LFT controller is performed as below:

$$\begin{aligned} x_K(k+1) &= A_K(\rho)x_K(k) + B_K(\rho)e(k) \\ \delta(k) &= C_K(\rho)x_K(k) + D_K(\rho)e(k) \end{aligned} \qquad (15)$$

where $x_K(k) \in \mathbb{R}^8$ is the state space vector of the LFT controller and, given the measurement $\rho(k)$ which updates the matrix $\Delta(\rho)$, the parameter-dependent matrices are calculated as such:

$$A_K(\rho) = A_K + B_{K_\Delta}\Lambda(\rho)C_{K_\Delta} \in \mathbb{R}^{8\times 8}$$
$$B_K(\rho) = B_{K_1} + B_{K_\Delta}\Lambda(\rho)D_{K_\Delta 1} \in \mathbb{R}^{8}$$
$$C_K(\rho) = C_{K_1} + D_{K_{1\Delta}}\Lambda(\rho)C_{K_\Delta} \in \mathbb{R}^{1\times 8} \qquad (16)$$
$$D_K(\rho) = D_{K_{11}} + D_{K_{1\Delta}}\Lambda(\rho)D_{K_{\Delta 1}} \in \mathbb{R}$$
$$\Lambda(\rho) = \Delta(\rho)(I - D_{K_{\Delta\Delta}}\Delta(\rho))^{-1}$$

5.1 Simulation result on lane change

The lane change situation can be simulated when the vehicle has to converge to the desired trajectory from an initial lateral offset. Fig. 8, 9 shows the convergence of the vehicle starting from 3 meters distance for $v_x = 10\ m/s, 15\ m/s$ and the look-ahead distance is chosen as $L = 30\ m, 60\ m$ respectively.

As it can been seen from the evolution of the lateral deviation, the vehicle converges smoothly to the desired trajectory for both speeds and remains always at that lane.
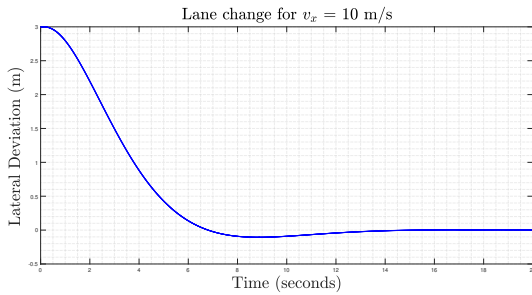

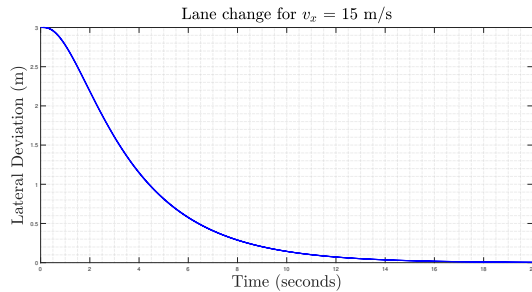Fig. 8. Vehicle response during lane change for $v_x = 10\ m/s$

Fig. 9. Vehicle response during lane change for $v_x = 15m/s$

5.2 Simulation results on lane tracking

In the case of lane tracking, as a simulation scenario is used a straight lane which continues to a turn of radius $R = 100m$ and then to a straight lane again. Fig. 10, 11 show the lateral deviation of the vehicle for speeds $v_x = 10, 15\ m/s$ and look-ahead distances $L = 15m, 20m$ accordingly.

The aforementioned figures show that the LFT controller is able to perform well during the turn without allowing big lateral errors at the center of gravity of the vehicle.

6. SIMULATION OF THE INTEGRATED CONTROL SCHEME WITH THE LFT CONTROLLER AND THE COMMAND GOVERNOR

This section presents the simulation results where the tracking controller is able to perform a dynamic maneuver at $v_x =$
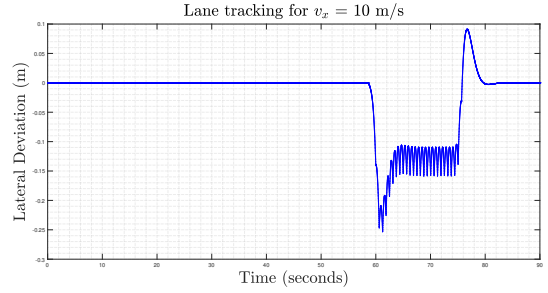

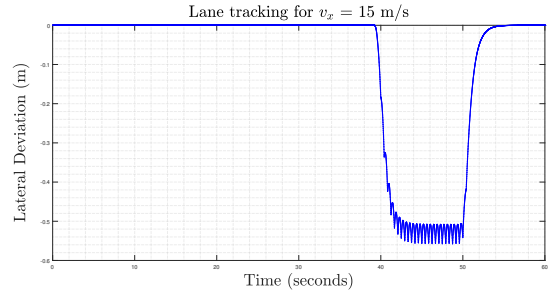Fig. 10. Vehicle response during lane tracking for $v_x = 10m/s$

Fig. 11. Vehicle response during lane tracking for $v_x = 15m/s$

$15\ m/s$ where the integrated control scheme of the LPV/LFT controller with the CG from Fig. 7 is implemented. For the parameters of Renault Zoe, is calculated that $\delta_{max} = 40$ degrees.

The QP optimization problem (13) is solved online using CVX-GEN (Mattingley and Boyd (2012)). The prediction horizon is chosen $N = 10$ and $\mathscr{D}_v = 0.01$.

The validity of the proposed method is proven by the simulation results, where the vehicle starts from an initial lateral offset of $3m$. The trajectory of the vehicle is shown in Fig. 12 where the vehicle is able to reach fast the desired trajectory without allowing significant overshoots.

Fig. 13 shows the applied steering command. It respects the maximum selected value without overshooting and consequently enables the fast lane change maneuver. Fig. 14 presents the comparison of the different yaw rates. The virtual yaw rate reference $v(k)$, computed online, makes feasible the vehicle to perform the maneuver via tracking the desired yaw-rate reference $r(k)$ when the steering wheel angle is between the "safe" bounds.
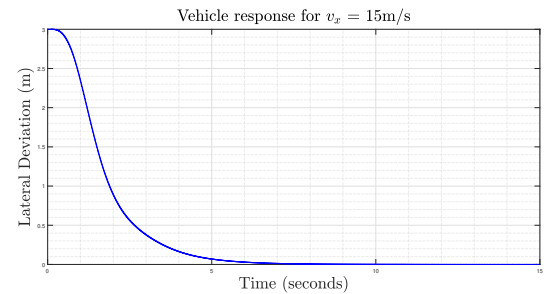

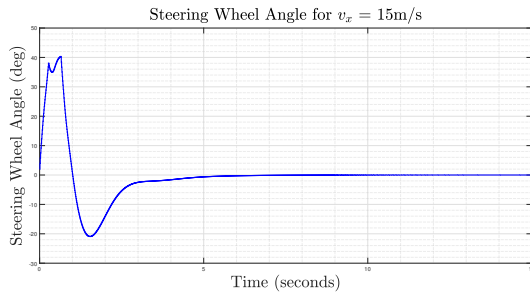Fig. 12. Vehicle response of the Governed system for $v_x = 15m/s$.

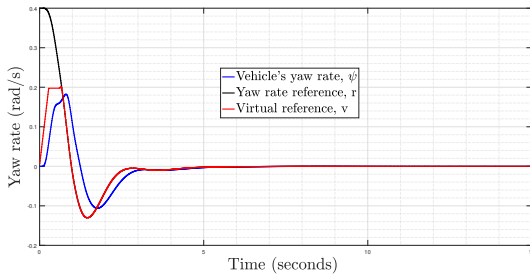Fig. 13. Steering wheel angle of the Governed system for $v_x = 15m/s$.

Fig. 14. Yaw rate comparison of the governed system for $v_x = 15m/s$.

7. CONCLUSION

This paper presents an LPV/LFT steering controller which is able to perform different tasks for a range of speeds. The controller is equipped with a command governor that keeps it in a "safe" region of steering commands by solving online a QP problem. Hence, the closed-loop system is able to perform a dynamic maneuver without leading the vehicle to instability.

Future works include the experimental validation of the proposed methodology on the real Renault Zoe vehicle for different speeds in order to investigate the limits of the vehicle. Another future step may be the experimental validation of the proposed methodology where more state constraints are included as the lateral speed of the vehicle during fast lane-change maneuvers for different velocities.

ACKNOWLEDGEMENTS

REFERENCES

Apkarian, P. and Gahinet, P. (1995). A convex characterization of gain-scheduled h_∞ controllers. *IEEE Transactions on Automatic Control*, 40(5), 853–864.

Beal, C.E. and Gerdes, J.C. (2012). Model predictive control for vehicle stabilization at the limits of handling. *IEEE Transactions on Control Systems Technology*, 21(4), 1258–1269.

Biannic, J.M., Apkarian, P., and Garrard, W.L. (1997). Parameter varying control of a high-performance aircraft. *Journal of Guidance, Control, and Dynamics*, 20(2), 225–231. doi: 10.2514/2.4045.

Cockburn, J.C. and Morton, B.G. (1997). Linear fractional representations of uncertain systems. *Automatica*, 33(7), 1263–1271.

Corno, M., Panzani, G., Roselli, F., Giorelli, M., Azzolini, D., and Savaresi, S.M. (2020). An lpv approach to autonomous vehicle path tracking in the presence of steering actuation nonlinearities. *IEEE Transactions on Control Systems Technology*, 1–9. doi:10.1109/TCST.2020.3006123.

Garone, E., Di Cairano, S., and Kolmanovsky, I. (2017). Reference and command governors for systems with constraints: A survey on theory and applications. *Automatica*, 75, 306–328.

Hjartarson, A., Seiler, P., and Packard, A. (2015). Lpvtools: A toolbox for modeling, analysis, and synthesis of parameter varying control systems. *IFAC-PapersOnLine*, 48(26), 139–145. 1st IFAC Workshop on Linear Parameter Varying Systems LPVS 2015.

Hoffmann, C. and Werner, H. (2015). A survey of linear parameter-varying control applications validated by experiments or high-fidelity simulations. *IEEE Transactions on Control Systems Technology*, 23(2), 416–433. doi: 10.1109/TCST.2014.2327584.

Kapsalis, D., Sename, O., Milanés, V., and Martinez, J.J. (2020). Gain-scheduled steering control for autonomous vehicles. *IET Control Theory & Applications*, 14(20), 3451–3460.

Kapsalis, D., Sename, O., Milanes, V., and Molina, J.J.M. (2021). Design and experimental validation of an lpv pure pursuit automatic steering controller. In *16th IFAC Symposium on Control in Transportation Systems*.

Kogiso, K. and Hirata, K. (2006). Reference governor for constrained systems with time-varying references. In *2006 IEEE International Conference on Multisensor Fusion and Integration for Intelligent Systems*, 359–364. IEEE.

Marcos, A., Bennani, S., Roux, C., and Valli, M. (2015). Lpv modeling and lft uncertainty identification for robust analysis: application to the vega launcher during atmospheric phase. *IFAC-PapersOnLine*, 48(26), 115 – 120. 1st IFAC Workshop on Linear Parameter Varying Systems LPVS 2015.

Mattingley, J. and Boyd, S. (2012). Cvxgen: A code generator for embedded convex optimization. *Optimization and Engineering*, 13(1), 1–27.

Pacejka, H. (2005). *Tire and vehicle dynamics*. Elsevier.

Packard, A. (1994). Gain scheduling via linear fractional transformations. *Systems & control letters*, 22(2), 79–92.

Paden, B., Čáp, M., Yong, S.Z., Yershov, D., and Frazzoli, E. (2016). A survey of motion planning and control techniques for self-driving urban vehicles. *IEEE Transactions on intelligent vehicles*, 1(1), 33–55.

Rajamani, R. (2011). *Vehicle dynamics and control*. Springer Science & Business Media.

Saupe, F. and Pfifer, H. (2012). An observer based state feedback lft lpv controller for an industrial manipulator. *IFAC Proceedings Volumes*, 45(13), 337 – 342. 7th IFAC Symposium on Robust Control Design.

Skogestad, S. (2007). *Multivariable feedback control: analysis and design*, volume 2.

Tan, H.S. and Huang, J. (2014). Design of a high-performance automatic steering controller for bus revenue service based on how drivers steer. *IEEE Transactions on Robotics*, 30(5), 1137–1147.

Taylor, C.J., Košecká, J., Blasi, R., and Malik, J. (1999). A comparative study of vision-based lateral control strategies for autonomous highway driving. *The International Journal of Robotics Research*, 18(5), 442–453.